Sternlicht, H. (1965) *J. Chem. Phys. 42*, 2250-2251.
Vasavada, K. V., & Nageswara Rao, B. D. (1989) *J. Magn. Reson. 81*, 275-283.
Villafranca, J. J. (1984) *Phosphorous-31 NMR: Principles and Applications* (Gorenstein, D. G., Ed.) pp 155-174, Academic, New York.
Virden, R., Watts, D. C., & Baldwin, E. (1965) *Biochem. J. 94*, 536-544.

^{1}H NMR Structural Characterization of a Recombinant Kringle 2 Domain from Human Tissue-Type Plasminogen Activator†

In-Ja L. Byeon,‡ Robert F. Kelley,§ and Miguel Llinás*,‡
Department of Chemistry, Carnegie Mellon University, Pittsburgh, Pennsylvania 15213, and Biomolecular Chemistry Department, Genentech, Inc., South San Francisco, California 94080
Received May 3, 1989; Revised Manuscript Received July 6, 1989

ABSTRACT: The kringle 2 domain of human tissue-type plasminogen activator (t-PA) has been characterized via ^{1}H NMR spectroscopy at 300 and 620 MHz. The experiments were performed on the isolated domain obtained by expression of the 174-263 portion of t-PA in *Escherichia coli* [Cleary et al. (1989) *Biochemistry 28*, 1884-1891]. The spectrum of t-PA kringle 2 is characteristic of a globular structure and shows overall similarity to that of the plasminogen (PGN) kringle 4. Spectral comparison with human and bovine PGN kringle 4 identifies side-chain resonances from Leu^{46}, which afford a fingerprint of kringle folding, and from most of the aromatic ring spin systems. Assignment of signals arising from the His^{13}, His^{48a}, and His^{64} side chains, which are unique to t-PA kringle 2, was assisted by the availability of a His^{64} → Tyr mutant. Ligand-binding studies confirm that t-PA kringle 2 binds L-lysine with an association constant K_a ~11.9 mM^{-1}. The data indicate that homologous or conserved residues relative to those that compose the lysine-binding sites of PGN kringles 1 and 4 are involved in the binding of L-lysine to t-PA kringle 2. These include Tyr^{36} and, within the kringle inner loop, Trp^{62}, His^{64}, Trp^{72}, and Tyr^{74}. Acid/base titration of aromatic singlets in the presence of L-lysine yields pK_a* ~6.25 and ~4.41 for His^{13} and His^{64}, respectively, and shows that the His^{48a} imidazole group does not protonate down to pH* ~4.3. Thus, the His^{48a} and His^{64} side chains are in solvent-shielded locations. As observed for the PGN kringles, the Trp^{62} indole group titrates with pK_a* ~4.60, which indicates proximity of the side chain to a titratable carboxyl group, most likely that of Asp^{57} at the binding site. Several labile NH protons of t-PA kringle 2 exhibit retarded H-exchange kinetics, requiring more than a week in ^2H_2O for full deuteration in the presence of L-lysine at 37 °C. This reveals that kringle 2 is endowed with a compact, dynamically stable conformation. Proton Overhauser experiments in ^1H_2O, centered on well-resolved NH resonances between 9.8 and 12 ppm, identify signals arising from the His^{48a} imidazole NH3 proton and the three Trp indole NH1 protons. A strong dipolar interaction was observed among the Trp^{25} indole NH1, the Tyr^{50} amide NH, and the His^{48a} imidazole CH2 protons, which affords evidence for an aromatic cluster in t-PA kringle 2 similar to that found at the hydrophobic kernel of PGN kringles. Overall, the data indicate a highly structured conformation for the recombinant t-PA kringle 2 that is closely related to that of the previously investigated PGN kringles 1, 4, and 5.

Tissue-type plasminogen activator (t-PA)[1] is a serine protease that converts the proenzyme plasminogen (PGN) into plasmin, which, in turn, efficiently degrades the fibrin network of blood clots (Collen, 1980). It consists of several distinct structural domains (Pennica et al., 1983): a finger domain homologous to fibronectin type 1 structures (Bányai et al., 1983), a growth factor domain resembling the mammalian epidermal growth factor (Doolittle et al., 1984), two kringle domains somewhat homologous to those in PGN, and a C-terminal proteolytic domain similar to the trypsin-like serine proteases (Patthy, 1985). The activation of PGN by t-PA is greatly enhanced by fibrin or its fragments (Hoylaerts et al., 1982; Rånby, 1982; Rijken et al., 1982). The acceleration seems to be due to the high affinity of these proteases for the fibrin matrix, ensuring that the activation occurs efficiently on the surface of a fibrin clot.

Systematic studies using domain deletion mutants suggest that the t-PA kringle 2 domain is involved in fibrin binding and, therefore, mediates the fibrin-dependent activation of PGN by t-PA (van Zonneveld et al., 1986a,b; Verheijen et al., 1986; Gething et al., 1988). These studies have also shown

† This research was supported by a grant-in-aid from the American Heart Association of Western Pennsylvania, Inc., by the U.S. Public Health Service, NIH Grant HL 29409, and by Genentech, Inc. The 620-MHz NMR facility is supported by NIH Grant RR 00292.
‡ Carnegie Mellon University.
§ Genentech, Inc.

[1] Abbreviations: bPGN, bovine plasminogen; CD, circular dichroism; CIDNP, chemically induced dynamic nuclear polarization; COSY, two-dimensional chemical-shift-correlated spectroscopy; FID, free induction decay; hPGN, human plasminogen; K_a, ligand-kringle equilibrium association constant; K2, kringle 2; K4, kringle 4; NOE, nuclear Overhauser effect; NOESY, two-dimensional NOE spectroscopy; PGN, plasminogen; pH*, glass electrode pH reading uncorrected for deuterium isotope effects; pK_a*, pK_a determined from acid/base titration in ^2H_2O, uncorrected for deuterium isotope effects; t-PA, human tissue-type plasminogen activator; u-PA, urokinase plasminogen activator; 2D, two dimensional.

0006-2960/89/0428-9350$01.50/0

that this domain exhibits lysine-binding properties. The fibrin/lysine-binding site on t-PA kringle 2 has, however, not been as thoroughly characterized as the binding site of PGN kringles 1, 4, and 5 (Winn et al., 1980; Trexler et al., 1982; Vâli & Patthy, 1984; Ramesh et al., 1987; Motta et al., 1987; Thewes et al., 1987). Furthermore, account should be taken that the t-PA kringles differ from the homologous domains found in PGN in that relative to the latter they contain three unique insertions: three residues between sites 44 and 45 and single residues between sites 48 and 49 and between sites 66 and 67. From this could originate structural perturbations that may lead to somewhat different NMR spectroscopic patterns and/or ligand-binding affinities or specificities. On the other hand, it is expected that the binding sites in the kringle homologues might exhibit similar properties simply because all these kringles share common basic elements of the lysine-binding site structure (Tulinsky et al., 1988a).

A number of ^{1}H NMR studies have been reported on PGN kringles 1, 4, and 5 (Llinás et al., 1983; Ramesh et al., 1986; Mabbutt & Williams, 1988; Thewes et al., 1988). Striking similarities among the spectra of these homologues have been observed, which indicate a close structural relatedness among the PGN kringles. The spectral correspondences have allowed us to analyze, identify, and confidently assign most of the aromatic and some of the aliphatic resonances. Valuable information about the ligand-binding site has been obtained by noting kringle resonances that are significantly perturbed by ligand (Llinás et al., 1985; Motta et al., 1987; Ramesh et al., 1987; Thewes, 1987; Petros et al., 1989). Magnetization transfer (Overhauser) experiments have helped to uncover points of contact between protein and ligand.

In this paper we report a first high-resolution ^{1}H NMR characterization of the t-PA kringle 2 in solution and present preliminary information on the binding site structure. The spectroscopic measurements were made on a t-PA kringle 2 obtained via expression of the individual domain in *Escherichia coli* (Cleary et al., 1989). The recombinant kringle 2 binds L-lysine ($K_a \sim 10.0$ mM^{-1}) and exhibits a CD spectrum similar to that of PGN kringle 4. Thus, a major goal of the present study is to establish the extent of conformational relatedness between the t-PA kringle 2 and those PGN kringles which have been studied by NMR. In the process, we have identified and assigned all of the aromatic and some aliphatic side-chain spin systems via two-dimensional spectroscopy backed by comparisons with similar data recorded for the PGN kringle 4 homologues. This enabled us to reach preliminary conclusions regarding the binding site structure.

Materials and Methods

t-PA kringle 2 domain (Figure 1) was expressed in *E. coli* and purified by using lysine–Sepharose affinity chromatography as previously described (Cleary et al., 1989). A mutant having His^{64} replaced with Tyr (designated H64Y) was constructed by using oligonucleotide-directed mutagenesis (R. F. Kelley, unpublished results) and was expressed and purified by using the same procedure. L-Lys and sodium phosphate were purchased from Aldrich Chemical Co. Deuterated solvent, ^2H_2O, was obtained from Merck, Sharp and Dohme Ltd (Montréal). Unless otherwise indicated, NMR samples of t-PA kringle 2 were prepared by dissolving the protein in either ^2H_2O or 90% ^1H_2O/10% ^2H_2O (which, for brevity, will henceforth be referred to as ^1H_2O) containing 0.05 M sodium phosphate to a final concentration of about 0.4–3.0 mM. The lowest concentration, 0.4 mM, was used at pH* 7.2, in absence of ligand, because of poor solubility under these conditions. pH* values quoted are uncorrected for deuterium isotope

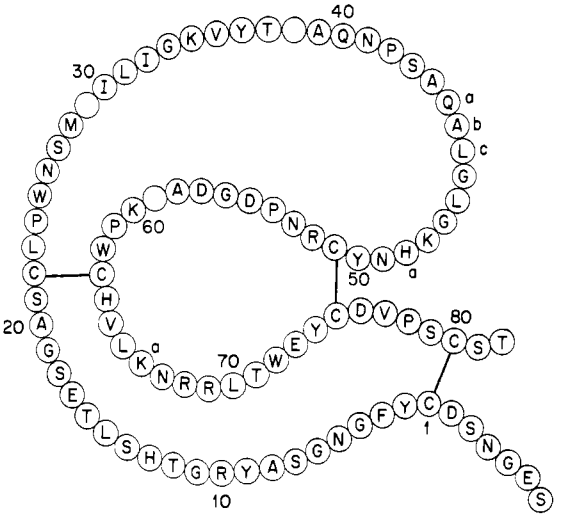

FIGURE 1: Recombinant kringle 2 domain of human t-PA: outline of the primary structure. The sequence corresponds to the Ser^{174}–Thr^{263} segment of native t-PA. Three deletions (at sites 29, 38, and 59) and five insertions (44a–44c, 48a, and 66a), have been introduced to facilitate comparison with PGN kringles. Site numbering, insertions, and deletions are based on homology with the PGN kringle 5 (Motta et al., 1987; Thewes et al., 1987) and differ slightly from that of Tulinsky et al. (1988a).

effects (Glasoe & Long, 1960). Solutions of the t-PA kringle 2 H64Y mutant were prepared by dissolving the protein in 0.14 M deuterated ammonium sulfate to a final concentration of about 0.5 mM. Human and bovine PGN kringle 4 were generated via elastase digestion of the parent protein and further purification by affinity chromatography on lysine–Sepharose (Sottrup-Jensen et al., 1978; Schaller et al., 1985). PGN kringle 4 was dissolved in salt-free ^2H_2O to a final concentration of 1.5 mM.

Proton NMR spectra were recorded at 300 MHz with a Bruker WM-300 spectrometer or at 620 MHz on the spectrometer of the NIH National NMR Facility for Biomedical Research at Carnegie Mellon University equipped with a Varian XL-400 console. Spectra recorded on the kringle sample in ^1H_2O were obtained by using the 1–1 hard pulse sequence (Clore et al., 1983). Chemical shifts are referred to the sodium 3-(trimethylsilyl)(2,2,3,3-$^2H_4$)propionate signal with *p*-dioxane as an internal standard (De Marco, 1977). One-dimensional NMR spectra were routinely acquired with quadrature detection over 16K data points to afford a digital resolution of 0.6 Hz (300 MHz) or 0.9 Hz (620 MHz). The residual $^1H^2HO$ signal was suppressed by selectively irradiating the proton transition for 1.2 s before sampling.

Acid/base titration data on t-PA kringle 2 were recorded in the presence of L-Lys, with [ligand]/[protein] = 3. The ligand was found to prevent precipitation of the protein around its isoelectric point, $5 < pH^* < 6.5$. The pH* was adjusted with small additions of 0.1 M ^{2}HCl or NaO^{2}H. pK_a* values for aromatic (His and Trp) singlets were derived by fitting the NMR data to the equation (Markley, 1975):

$$\Delta\delta = (\delta_{H^+} - \delta_{obs})/(\delta_{H^+} - \delta_{H^0}) = K_a^n/(K_a^n + [H^+]^n) \quad (1)$$

where K_a is the proton dissociation constant of the side chain, δ_{H^+}, δ_{H^0}, and δ_{obs} are the acid, base, and observed chemical shifts, respectively, and n is the Hill coefficient.

Two-dimensional COSY spectra (Wider et al., 1984) were acquired with 512 t_1 values and accumulations of 288 scans (at 300 MHz) or 64 scans (at 620 MHz) per t_1 spectrum. The spectral width was about 3400 Hz at 300 MHz or 7200 Hz at 620 MHz with 2K data points. Quadrature detection mode

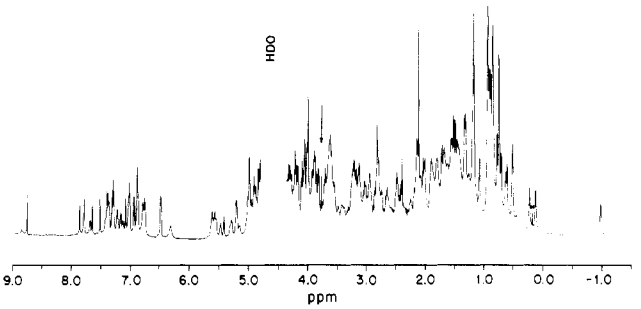

FIGURE 2: ^1H NMR spectrum of human t-PA kringle 2 at 620 MHz. Kringle 2 concentration ~1.5 mM, dissolved in ^2H_2O, 0.05 M sodium phosphate, pH* 4.5, 37.8 °C. The spectrum was recorded after exchange of labile hydrogen atoms for deuterium and is shown with slight resolution enhancement. The arrow points to the internal dioxane reference singlet: the asterisk (*) denotes a contaminant signal.

and appropriate phase cycling were utilized to select only N-type peaks (Bruker software package). The residual $^1H^2HO$ resonance was suppressed by gated irradiation during the relaxation delay of 2.3 s introduced between scans. Before Fourier transformation, the t_1 time domain was zero-filled to 1K, and FIDs were multiplied by appropriate weighing functions in both t_1 and t_2 dimensions to enhance resolution or sensitivity. Digital resolution in the final transformed spectrum was about 3.3 Hz (at 300 MHz) or 7.1 Hz (at 620 MHz) in both dimensions. The contour plots are shown in the absolute value mode after symmetrization.

Ligand binding of t-PA kringle 2 was studied by adding small volumes of a concentrated, preexchanged L-lysine solution to the kringle sample, which was dissolved in 0.4 mL of ^2H_2O containing 0.1 M sodium phosphate at pH* 7.2, 22 °C. Because of the low concentration of protein (~0.4 mM) required by the low solubility of kringle 2 under these conditions, accumulation of several thousand scans was required to obtain a spectrum with a satisfactory signal to noise ratio. The kringle–lysine association constant, K_a, was calculated after taking into account dilution effects (De Marco et al., 1982, 1987).

Truncated driven Overhauser experiments (Dubs et al., 1979) in ^1H_2O were performed by preirradiating a transition for 0.5 s before sampling with the 1–1 hard pulse. NOEs are shown as difference spectra (unperturbed minus perturbed) so that negative NOEs appear with positive amplitudes.

Results and Discussion

The 620-MHz ^1H NMR spectrum of t-PA kringle 2 dissolved in ^2H_2O is shown in Figure 2. The spectrum spans the -1 ppm $\lesssim \delta \lesssim 9$ ppm chemical shift range and exhibits features similar to those observed for the PGN kringles, such as (a) a generalized spread of aromatic signals over a wide chemical shift range, (b) presence of CH^α resonances low field shifted relative to the $^1H^2HO$ signal, and (c) methyl group protons resonating near −1 ppm. These features suggest a globular conformation with substantial secondary and/or tertiary structure for the isolated kringle 2 domain.

Figure 3B shows an expansion of the high-field methyl region of the t-PA kringle 2 spectrum. Two doublets, at 0.50 and −0.98 ppm, arise from a Leu side-chain spin system, as identified from a COSY experiment (not shown). By comparison with the spectrum of PGN kringle 4 (Figure 3A), these doublets are assigned to the δ,δ'-methyl groups of Leu[46]. This assignment is based on the observation that the Leu[46] residue, conserved in all the kringles sequenced to date, consistently yields a doublet at ~−1 ppm (Llinás et al., 1983, Thewes et al., 1987), thus affording a characteristic marker for kringle

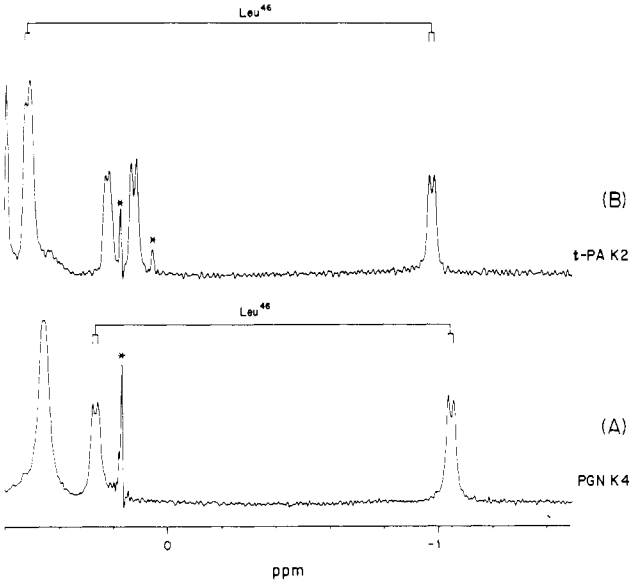

FIGURE 3: ^1H NMR spectra of homologous kringles at 300 MHz: high-field methyl region. (A) Human PGN kringle 4; (B) human t-PA kringle 2. Spectra were recorded in ^2H_2O, pH* 4.5, with (B) or without (A) 0.05 M sodium phosphate. Protein concentration ~ 1.5 mM, 37 °C. The spectra are shown resolution enhanced. An asterisk (*) is used to indicate contaminant signals.

identity and folding. A unique three-proton singlet in the aliphatic region, at 2.1 ppm (Figure 2), can be assigned to the Met[28] CH_3^ϵ group. The position and sharpness of the resonance indicate that the Met[28] side chain is rather mobile. In contrast, in PGN kringle 4 the Met[28] CH_3^ϵ group yields a broadened line shifted to 1.49 ppm, reflecting an interaction of the Met[28] side chain with the imidazole ring of His[33] (Petros et al., 1988a). The His[33] residue is replaced with a Gly residue in t-PA kringle 2. Thus, it is apparent that the environment of the Met[28] side chain in t-PA kringle 2 is somewhat different from that in PGN kringle 4.

Figure 4A shows the 5.5 ppm $< \delta <$ 12.8 ppm spectrum of t-PA kringle 2 dissolved in ^1H_2O in the presence of L-Lys. Besides displaying the aromatic CH resonances, this spectral region contains signals from exchangeable NH groups in peptidyl amides, Trp indole, and His imidazole groups. Upon dissolving the sample in ^2H_2O, the amplitudes of the NH resonances decay at various rates, reflecting ^1H–^2H exchange. The global kinetics of the process can be assessed by inspecting Figure 4B–D, where each spectrum represents a 10-h average starting 0.3 h (B), 32 h (C), and 168 h (D) after dissolving the protein in the deuterated solvent. It is apparent that while most labile NH signals disappear immediately at the start of the experiment (Figure 4B), a number of NH group exhibit slow exchange, in particular, a set of amides resonating within the 8.8–9.5 ppm range (Figure 4C). Among these, the most noticeable is the one at ~9 ppm (Figure 4D), which is only partially exchanged after a week. These data further indicate that the kringle has a rather compact globular conformation as resonances from slowly exchanging protons normally arise from intramolecular H-bonded and/or buried NH groups. In the absence of lysine (data not shown), full exchange deuteration of kringle 2 requires several days at pH* 7.2, 40 °C. In this context, it is interesting to recall that under identical conditions the PGN kringle 4 is fully deuterated within ~4 h (Hochschwender et al., 1983), which is indicative of a relatively more flexible structure. Thus, it is probably not fortuitous that the thermal stability of the t-PA kringle 2 is slightly higher than that of the PGN kringle 4 (Kelley & Cleary, 1989a).

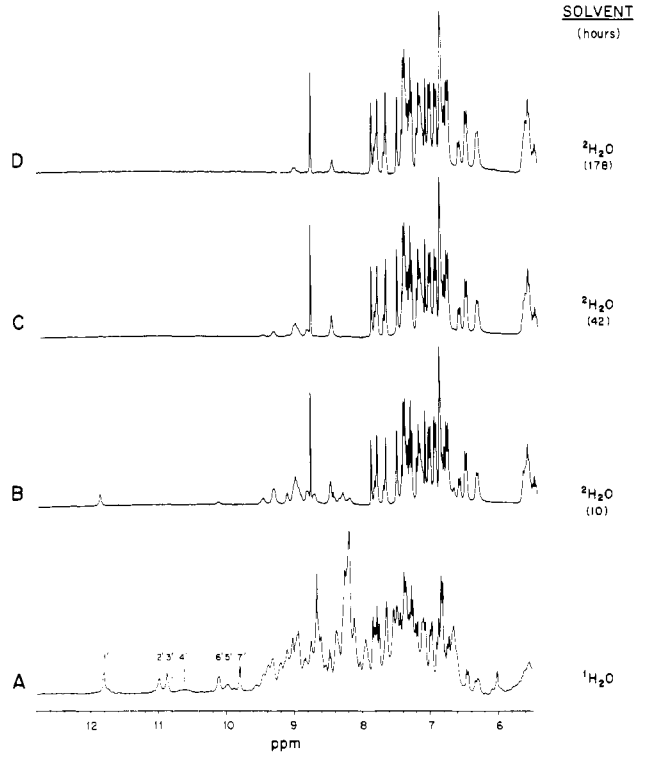

FIGURE 4: 300-MHz ^1H NMR spectra of t-PA kringle 2 in the presence of L-Lys: NH ^1H–^2H exchange in ^2H_2O. (A) Control spectrum in ^1H_2O, recorded by using the 1–1 hard-pulse technique (Clore et al., 1983). Other spectra were acquired from 10-h accumulation starting 0.3 h (B), 32 h (C), and 168 h (D) after dissolving the kringle sample in ^2H_2O. (A) 2 mM kringle 2 in ^1H_2O, pH 5.0, 37 °C; (B–D) 1.5 mM kringle 2 in ^2H_2O, pH* 4.5, 37 °C. All spectra are shown with the same resolution enhancement.

Chart I: Labeling of Aromatic Atom Sites

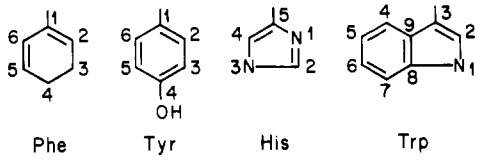

Histidyl Spectra. Figure 5A shows the aromatic region of the t-PA kringle 2 spectrum, recorded at pH* 7.2, 37 °C, after exhaustive exchange deuteration of NH sites. Kringle 2 has three Trp residues, at sites 25, 62, and 72, and three His residues, at sites 13, 48a, and 64 (Figure 1). Thus, nine singletlike peaks, arising from the three Trp indole CH2 groups (Chart I) and from the three pairs of His imidazole CH2/CH4 protons, are expected to show up in the aromatic spectrum. The peaks are numbered 1–9 according to their chemical shift ordering; on lowering the pH* to 4.5, they variously shift to low fields, with peaks 8 and 9 moving the most (Figure 5B). Resonances 8 and 9 are also observed to gradually lose intensity due to ^1H–^2H exchange against solvent ^2H_2O at neutral or alkaline pH*, thus indicating that they arise from His imidazole CH2 protons (Figure 5A).

Acid/base titration curves for the nine aromatic singlets are shown in Figure 6. Singlets 1 and 9 exhibit similar pH* profiles, yielding pK_a* ~4.41, which identifies the two peaks as arising from the same His ring spin system: His-III (H-III).[2] Upon acidification, singlet 9 exhibits a more pronounced shift (~2 ppm) relative to singlet 1 (~0.2 ppm), consistent with its assignment to an imidazole CH2 proton (Figure 5A). Solvent exchange deuteration of the His-III singlet 9 CH2 site slows down whenever a lysine-type ligand is added to the kringle solution. This indicates that the imidazole CH2 site

[2] Roman numerals are used to label aromatic side-chain spin systems, independent of their assignments to specific residues in the primary sequence.

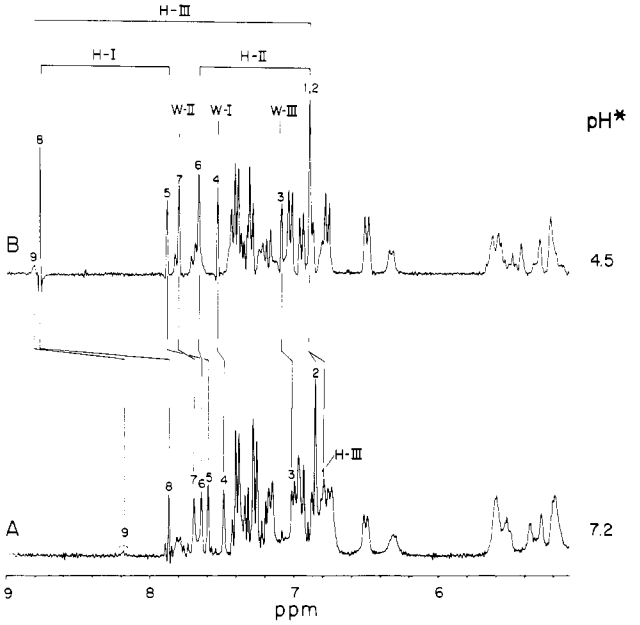

FIGURE 5: ^1H NMR spectra of t-PA kringle 2 at 300 MHz: acid/base perturbation of aromatic resonances. Spectra were recorded on samples dissolved in ^2H_2O, 0.05 M sodium phosphate, 37 °C, at pH* 7.2 (A) and 4.5 (B), after exchange of labile hydrogen atoms for deuterium. Kringle 2 concentration was 0.5 mM (A) or 1.5 mM (B). His and Trp singlets are numbered 1–9 according to their chemical shift ordering at pH* 7.2 (A). His imidazole spin systems are indicated as H-I (His[13]), H-II (His[48a]), and H-III (His[64]). Trp indole H2 singlets are labeled W-I (Trp[25]), W-II (Trp[62]), and W-III (Trp[72]). Singlets 8 and 9 exhibit reduced amplitudes in (A) due to exchange deuteration in ^2H_2O.

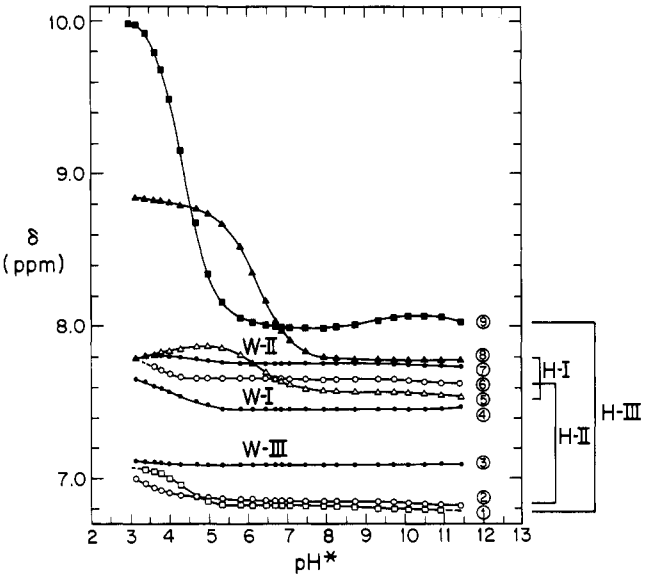

FIGURE 6: Acid/base titration of aromatic singlets in the ^1H NMR spectrum of t-PA kringle 2 in the presence of L-Lys. Data points are labeled according to the singlet numbering used in Figure 5. The data were obtained from spectra recorded at 300 MHz, 37 °C, on solutions of kringle 2 prepared in ^2H_2O with labile hydrogen atoms allowed to exchange with solvent prior to measurement: squares, H-III; circles, H-II; triangles, H-I; open symbols, H4 resonances; filled symbols, H2 resonances. Dots denote Trp H2 data. The derived pK_a* values are 6.25 for H-I (His[13]), 4.41 for H-III (His[64]), and 4.6 for W-II (Trp[62]). [Ligand]/[kringle 2] ~ 3.

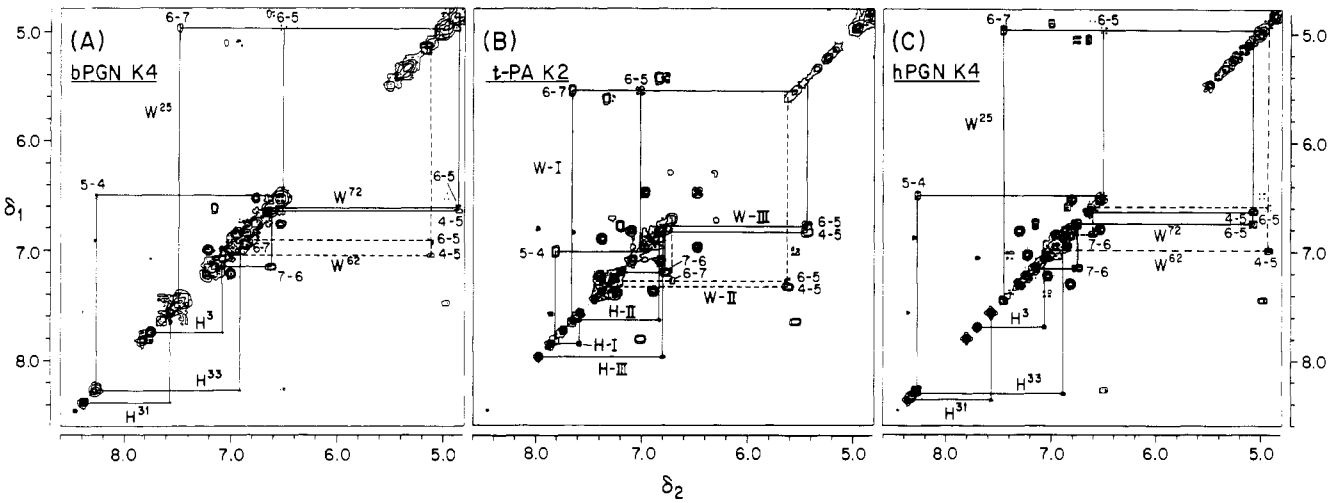

FIGURE 7: 300-MHz COSY spectra of kringle homologues in the presence of L-Lys: His and Trp aromatic spin systems. (A) Bovine PGN kringle 4, (B) human t-PA kringle 2, (C) human PGN kringle 4. Scalar connectivities for the His and Trp side chains are indicated by solid lines except for W-II (Trp^{62}), which is denoted by dashed lines. Off-diagonal Trp cross-peaks, labeled by two-digit numbers, represent pairs of ring protons connected via scalar coupling. The "matrix" convention (first digit labels row proton, second digit labels column proton) is used to mark individual connectivities. The spectra are shown resolution enhanced with a sine bell function in both dimensions. Kringle concentration ~ 1.5 mM, [ligand]/[kringle] ~ 3. Protein solutions are in ^2H_2O, pH* 7.2, 37 °C, salt free (A and C) or in 0.1 M sodium phosphate (B).

is somewhat exposed but becomes shielded from solvent upon ligand binding. The His-III imidazole spin system was assigned to His^{64} by comparison with a spectrum of the H64Y mutant kringle 2 domain (not shown).

The pH* profiles for singlets 5 and 8 (Figure 6) show similar shapes (pK_a* ~6.25). Therefore, we assign them to the same His ring spin system, labeled His-I (H-I). The relatively larger overall shift upon acidification exhibited by singlet 8 is consistent with its identification as an imidazole CH2 resonance as suggested above. However, in contrast to what is observed for the His-III (His^{64}) CH2 resonance, addition of ligand does not affect the chemical shift or the exchange kinetics of the His-I imidazole CH2 proton. Therefore, the His-I side chain is probably on the protein surface and is removed from the lysine-binding site. Despite this assertion, it is clear from the pH titration curve that the His-I side chain experiences some kind of intramolecular interaction with other protein groups as it exhibits a chemical shift acid/base dependence at pH* $\lesssim$4.5 (Figure 6). As discussed below, His-I should be assigned to His^{13}. On the other hand, NOE experiments (not shown) reveal that the His^{13} imidazole ring is in close contact with the Cys^{75} CH^{β} group, which affords an important constraint to determine the protein folding. Thus, it is likely that the low pH effect on its chemical shift reflects an acid-induced unfolding process that leads to a change in the local magnetic environment of His^{13}.

Peaks 2 and 6 can be assigned to the spin system of the remaining His imidazole ring (His-II) on the basis of a COSY connectivity between the CH2 and CH4 protons, which is readily detected despite the small J coupling (Figure 7B). Cross-peaks between signals 1 and 9 (His-III), and 5 and 8 (His-I), are also apparent in the 2D spectrum, which verifies the imidazole CH2–CH4 pairing scheme proposed above. His-II singlets 2 and 6 also exhibit a similar alkali insensitivity above pH* ~4.3 (Figure 6), and neither proton undergoes ^1H–^2H exchange in ^2H_2O. However, on the basis of 2D NOESY experiments (not shown), we have unambiguously assigned singlets 2 and 6, respectively, to the CH4 and CH2 imidazole protons.

Unlike the His-I and His-III side chains, the His-II ring would appear to be located in a highly shielded position within the domain structure. On the basis of knowledge regarding the relative exposure of various segments of the kringle sequence (Ramesh et al., 1987; Tulinsky et al., 1988b), one can tentatively assign the internal residue, His-II, to His^{48a} and the solvent-exposed one, His-I, to His^{13}.

Tryptophanyl Spectra. The identification and assignment of the t-PA kringle 2 Trp aromatic spectrum are more straightforward than the assignment of the His resonances since the three Trp residues are retained on going from PGN kringle 4 to t-PA kringle 2 whereas the His residues are not. Furthermore, since all His imidazole CH signals have been identified, the remaining singlets 3, 4, and 7 must arise from three Trp indole CH2 protons, labeled Trp-III (W-III), Trp-I (W-I), and Trp-II (W-II), respectively (Figure 5).

As shown in Figure 6, the Trp-II singlet 7 slightly titrates at pH <5.5 with pK_a* ~4.6 and is the most low-field-shifted. In kringles 1, 4, and 5 of PGN, the Trp^{62} indole CH2 resonance is the most low-field-shifted among the Trp singlets and consistently titrates with $4 \lesssim pK_a^* \lesssim 5$, suggesting interaction with a neighboring acidic side chain (De Marco et al., 1985b; Motta et al., 1986b; Thewes et al., 1987). On this basis, singlet 7 of the t-PA kringle 2 is assigned to the Trp^{62} indole CH2 group. The acid/base sensitivity of the Trp-II CH2 resonance is in agreement with the appearance of a cross-peak connecting between Trp-II NH1 and Asp^{57} β-protons in NOESY spectra of t-PA kringle 2. The identification of the Asp^{57} connectivity is based on a number of 2D experiments aimed at complete sequential assignments for kringle 2 (not shown).

In PGN kringle 4, the CH2 resonance of the Trp^{72} indole group does not exhibit any significant response to pH changes and, relative to the Trp^{25} and Trp^{62} singlets, appears shifted to a higher field position (De Marco et al., 1985b). In t-PA kringle 2, the Trp-III singlet 3 exhibits these same features. Hence, singlet 3 is assigned to the Trp^{72} indole CH2 proton. By default, singlet 4 should arise from Trp^{25}. However, it should be noted that while in the t-PA kringle 2 the Trp^{25} singlet frequency shifts on lowering the pH below ~5.0 (Figure 6), in the PGN kringles it is mostly unperturbed by acidic conditions. As shown by Overhauser experiments (discussed below), the Trp^{25} NH1 proton in t-PA kringle 2 is located close to the His^{48a} (H-II) CH2 site (→ singlet 6) so that the protonation state of the His^{48a} imidazole group may contribute to the shift of the Trp^{25} side-chain resonances. A

comparison of the near-UV CD spectra observed for t-PA kringle 2 and PGN kringle 4 suggests that one or more Trp residues of t-PA kringle 2 are in a more polar environment than in PGN kringle 4 (Cleary et al., 1989).

The COSY spectrum enables us to map the scalar J connectivities among the Trp indole multiplets of t-PA kringle 2 (Figure 7B). Figure 7 also shows the aromatic COSY spectra of the bovine and human PGN kringle 4 domains (A and C, respectively). Although some variability is evident, comparison with the homologous kringle 4 spectra greatly assists in assigning the Trp ring spin systems of the t-PA kringle. Two characteristics distinguish the Trp-I from the Trp-II and Trp-III spin systems of t-PA kringle 2: (a) the overall chemical shift range of the Trp-I indole resonances (~2.25 ppm) is wider than that observed for Trp-II or Trp-III (<1.80 ppm); (b) the indole CH4 and CH7 doublets of Trp-I are low-field-shifted relative to the aromatic multiplets from the other two Trp spin systems (Figure 7B). Such characteristics are also displayed by Trp^{25} in the bovine and human kringle 4 spectra (Figure 7A,C). Indeed, although the chemical shift range spanned by the Trp-I indole resonances in the t-PA kringle is narrower than for Trp^{25} in the homologues, the overall Trp-I COSY connectivity pattern agrees well with that of Trp^{25} in the two PGN kringles (Figure 7).

Among the Trp residues in t-PA kringle 2, Trp-III exhibits the most distinct spectrum, readily visualized because of its more intense cross-peaks (Figure 7B). For the Trp indole spin systems of the PGN kringles, the most intense cross-peaks are displayed by Trp^{72}, consistent with a rather mobile side chain. Chemical modification (Hochschwender & Laursen, 1981) and photo-CIDNP (De Marco et al., 1989) experiments on PGN kringle 4 indicate that the Trp^{72} side chain is accessible to solvent. Also, the COSY connectivity pattern of both the Trp-III spin system in t-PA kringle 2 and the Trp^{72} spin system in the PGN kringle 4 variants is similar (Figure 7). Therefore, we assign Trp-III to Trp^{72}. By elimination, the Trp-II spin system should arise from Trp^{62}.

The absolute assignment of resonances to specific indole group protons (as indicated in Figure 7B) was achieved via Overhauser experiments in ^1H_2O whereby the indole NH1 transition was irradiated and NOEs were observed on the CH2 singlet and the CH7 doublet from the same ring. These experiments, which are discussed below, also unambiguously establish the correspondence between indole CH singlets and multiplets for the Trp residues.

Shifted NH Resonances. A number of NH resonances, labeled 1′–7′, appear shifted and well resolved in the 9.6 ppm $\lesssim \delta \lesssim$ 12.0 ppm region in ^1H_2O (Figure 4A). Often, such signals arise from His or Trp aromatic side chains. In order to identify the origin of these signals, a number of Overhauser experiments were implemented. Figure 8F illustrates an experiment where the sharp peak 7′ transition at 9.78 ppm was irradiated. Strong NOEs on the Trp^{72} (W-III) indole doublet at 7.23 ppm and a singlet at 7.13 ppm are observed. This indicates that 7′ stems from the Trp^{72} indole NH1 proton, while the doublet and singlet arise from the CH7 and CH2 protons, respectively, on the same indole ring. Similarly, irradiation of transition 1′ at 11.81 ppm—arising from a proton that exhibits a retarded ^1H–^2H exchange in ^2H_2O (Figure 4B)—generates NOEs on the Trp^{25} (W-I) indole CH2 singlet and CH7 doublet and on the His^{48a} (H-II) CH2 singlet (Figure 8A). The latter two, which overlap under the experimental conditions, become better resolved at 67 °C (Figure 8, insert above spectrum A). This experiment identifies the Trp^{25} indole NH1 (peak 1′), CH2, and CH7 resonances. Indeed, peak 1′

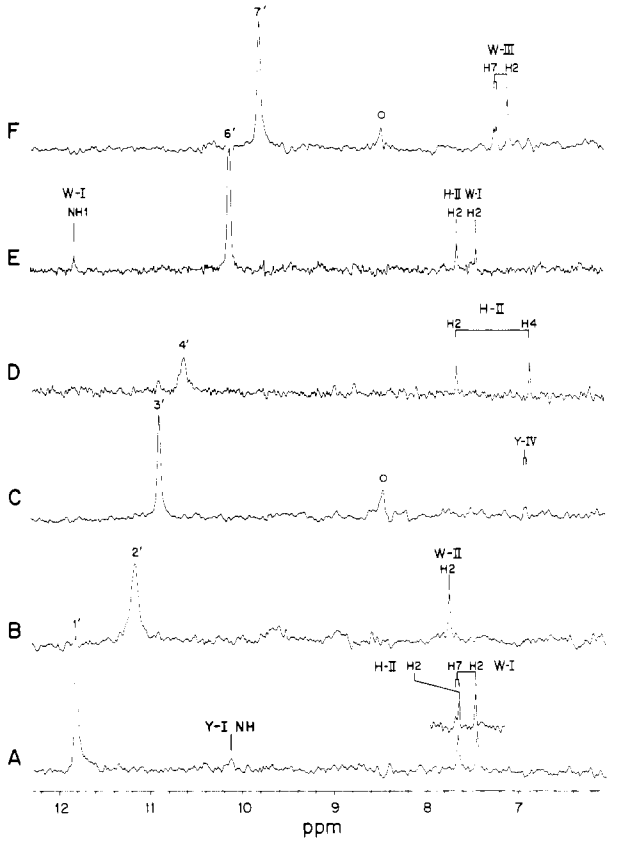

FIGURE 8: t-PA kringle 2 in the presence of L-lysine: proton Overhauser experiments at 300 MHz. (A–F) NOE difference spectra resulting from irradiating NH resonances 1′–4′, 6′, and 7′ (see Figure 4A). The correspondence between identified NOE signals and proton positions in the aromatic rings is indicated. A preirradiation pulse was applied for 0.5 s on- and off-resonance before sampling; 2.3-s recycling time. Each NOE spectrum results from in-memory subtraction of equal numbers of off- and on-resonance irradiation experiments, so that negative NOEs show with positive amplitude. Kringle dissolved in ^1H_2O, concentration ~ 3 mM, pH 6.0, 37 °C, [L-Lys]/[kringle 2] ~ 4. The insert (above spectrum A) is the same experiment as in (A) but at 67 °C pH 7.28. Experimental artifacts are denoted by an open circle (O).

is similar to resonances observed in spectra of PGN kringles 1, 4, and 5, where they have also been assigned to the Trp^{25} NH1 resonance (Motta et al., 1986a,b; Thewes et al., 1988). The observation of a large NOE on the His^{48a} (H-II) imidazole CH2 singlet indicates that the Trp^{25} and His^{48a} side chains lie close.

The selective irradiation of peak 2′ at 11.15 ppm elicits a strong NOE on the Trp^{62} (W-II) indole CH2 singlet, so peak 2′ can be identified as the Trp^{62} aromatic NH1 signal (Figure 8B). However, the expected NOE on the CH7 doublet is not observed. This most likely reflects other competing dipolar interactions which drain the excess CH7 magnetization and dominate its T_1 relaxation kinetics. Thus, the experiments illustrated in Figure 8, in combination with the COSY connectivities, unambiguously assign each of the Trp^{25} and Trp^{72} aromatic resonances, as labeled in Figure 7B. For Trp^{62}, whose CH7 doublet was undetected in the Overhauser experiment, the indole proton assignment is inferred from comparisons with the homologous kringle 4 spectra (Figure 7).

The broad NH peak 4′ at 10.61 ppm (Figure 4A) narrows and becomes visible only at pH ~6, which suggests it represents a His imidazole NH resonance. Irradiation of this peak yields strong NOEs on the two His^{48a} (H-II) ring singlets (Figure 8D). This experiment both assigns peak 4′ to the His^{48a} imidazole NH3 proton and further substantiates the

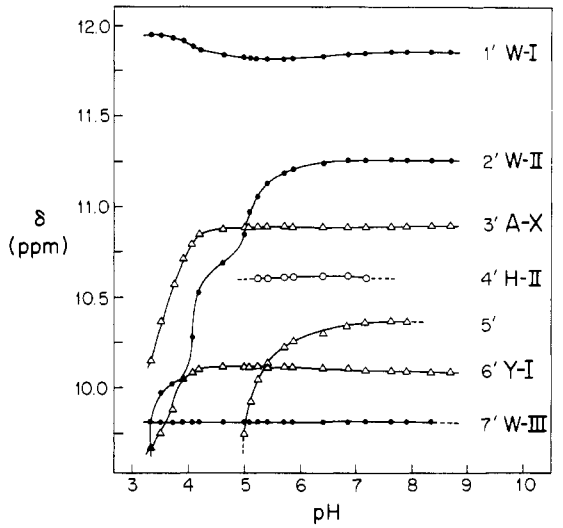

FIGURE 9: Acid–base titration profile of low-field NH proton resonances in the ^1H NMR spectrum of t-PA kringle 2 in the presence of L-Lys. Data labeling and experimental conditions are as for Figure 11.

pairing of CH singlets 2 and 6 to the same ring spin system (Figure 5–7). Also informative is the result of irradiating peak 6′ (a doublet) at 10.12 ppm (Figure 8E), which yields NOEs on the His^{48a} (H-II) imidazole CH2 peak and the Trp^{25} (W-I) indole CH2 and NH1 resonances (Figure 8E). As is the case for the Trp^{25} NH1 peak 1′, signal 6′ arises from an NH which exhibits retarded exchange in ^2H_2O (Figure 4B). Combined with the NOE data, this observation suggests that peak 6′ arises from an internal NH group that is in close proximity to buried residues, Trp^{25} (W-I) and His^{48a} (H-II). The comparable intensities of three NOE peaks illustrated in Figure 8E suggest that the peak 6′ proton is positioned approximately equidistant from the Trp^{25} (W-I) NH1, CH2, and His^{48a} (H-II) CH2 protons. From 2D experiments in ^1H_2O, we have identified peak 6′ as the amide proton of Tyr^{50}. Thus, the appearance of this NH peak at an unusual low-field position may be attributed to ring current effects from the neighboring Trp^{25} and/or His^{48a} aromatic groups. The close proximity between Trp^{25} and Tyr^{50} is consistent with the crystallographic structure of the prothrombin kringle 1, where the Phe^{50} ring is ~4.2 Å (interproton closest distance) from the Trp^{25} indole group (Park & Tulinsky, 1986). Finally, an Overhauser experiment in which the NH proton 3′ transition at 10.89 ppm was irradiated yielded a small NOE on an aromatic CH doublet, identified below as Tyr^{74} (Y-IV) (Figure 8C). On the basis of 2D NMR information, NH resonance 3′ has been identified as arising from the Ala^{58} amide group (data not shown).

The chemical shifts of the seven resolved NH resonances of t-PA kringle 2 in the presence of lysine are plotted versus pH in Figure 9. Although the Trp^{72} NH1 resonance (peak 7′) broadens extensively under alkaline conditions, its chemical shift is essentially pH-insensitive. This is consistent with the invariant pH titration profile of the Trp^{72} indole CH2 signal (singlet 3, Figure 6). In contrast, the Trp^{62} NH1 resonance (peak 2′) is most sensitive to pH changes: it exhibits pronounced high-field shifts at pH <6 yielding two inflections at pH ~5.1 and ~4.1. The one at pH 5.1 is consistent with pK_a^* = 4.6 determined for the Trp^{62} CH2 resonance (singlet 7, Figure 6) once account is taken of the ~0.4 pH unit correction due to the $^2H/^1H$ isotope effect (Glasoe & Long, 1960). This indicates that both Trp^{62} NH1 and CH2 resonances are influenced by the same neighboring (Asp^{57}) ionizable group. The second inflection, of pK_a ~4.1, suggests a further interaction with a titratable group of low pK_a. The Trp^{25} NH1 resonance (peak 1′) is relatively pH-insensitive within the alkaline-to-neutral range; acidification below pH ~5 results in a small shift to low field. Again, the pH response of this resonance correlates well with that of the CH2 signal from the same indole group (peak 4 in Figure 6). Notice that amide NH peaks 3′ (Ala^{58}) and 6′ (Tyr^{50}) shift at pH ≲4. It is likely that these perturbations reflect incipient local unfolding(s).

No attempt was made to irradiate the resonance 5′ transition as, under the experimental conditions (pH 6.0), its line width made it difficult to achieve satisfactory results. However, the pH dependence of resonance 5′ suggests that it may stem from a His imidazole NH3 proton (Figure 9). Since resonance 4′ has been assigned to His^{48a}, it is likely that 5′ arises from His^{64} (His III) as this residue starts to titrate at pH ≲6 (Figure 6), in agreement with the curve for 5′ in Figure 9.

Tyrosyl Spectra. t-PA kringle 2 contains five Tyr residues among which Tyr^{36} is unique to this domain, whereas Tyr^2, Tyr^9, Tyr^{50}, and Tyr^{74} are conserved in human PGN kringle 4. (The latter also has a Tyr residue at site 41.) Figure 10 shows aromatic 300-MHz COSY spectra of the human t-PA kringle 2 (A) and PGN kringle 4 (B). Cross-peaks from four rapidly rotating Tyr rings, labeled Tyr-I (Y-I), Tyr-II (Y-II), Tyr-III (Y-III), and Tyr-IV (Y-IV), can be observed in the spectrum of kringle 2. Comparison of Figure 10 spectra A and B leads to assigning the Tyr-IV spin system to Tyr^{74}. This assignment is further supported by an Overhauser experiment (not shown) where irradiation of the Trp^{62} (Trp-II) indole CH2 singlet produces NOEs on the Tyr-IV aromatic doublets: identical NOEs, connecting Trp^{62} and Tyr^{74}, have been observed for PGN kringles 1, 4, and 5 (Motta et al., 1987; Ramesh et al., 1987; Thewes et al., 1988). Thus, the NMR evidence would indicate that the microenvironment of Tyr^{74} is largely conserved among the homologous domains.

The Tyr-II cross-peak (6.50, 6.97 ppm) compares well with that of Tyr^2 (6.55, 6.82 ppm) in the human PGN kringle 4. This suggests assigning Tyr-II to Tyr^2. Since Tyr-V is assigned to Tyr^9 (see below), the two other Tyr spin systems, Tyr-I and Tyr-III (Figure 10A), should arise from Tyr^{50} and Tyr^{36}. In PGN kringles, the conserved residue, Tyr^{50}, consistently exhibits a pattern of COSY cross-peaks close to the diagonal (Figure 10B). In the t-PA kringle 2, neither Tyr-I nor Tyr-III exhibit such characteristics. However, sequential assignment experiments (in progress) conclusively identify Tyr-III as Tyr^{36} and Tyr-I as Tyr^{50}. Thus, the Tyr^{50} ring in t-PA kringle 2 experiences a rather different environment from the one it encounters in the PGN kringles. It is likely that the shifted Tyr^{50} spectrum reflects the close contact, in the t-PA kringle 2, between its side chain and the His^{48a} (H-II) imidazole group as indicated by the NOE evidence discussed above.

Finally, the Tyr-V (Y-V) ring spin system, which is not detected at 300 MHz, pH* 7.2 (Figure 10A), becomes visible as an ABCD system, yielding two distinct ortho–meta COSY cross-peaks, at 620 MHz, pH* 4.5, whether ligand free (Figure 11A) or in the presence of L-Lys (Figure 11B). A Tyr spectrum containing four one-proton doublets reveals a slow flip dynamics for the corresponding phenol ring. A similar pattern has been observed for Tyr^9 in PGN kringle 4 homologues (De Marco et al., 1985b; Ramesh et al., 1986; Petros et al., 1988b). Therefore, we assign Tyr-V in t-PA kringle 2 to Tyr^9. It is also apparent that the Tyr-V aromatic chemical shifts in the t-PA kringle are strikingly close to those that Tyr^9 exhibits in the homologous PGN domains. This indicates that environmental features defining the Tyr^9 locus are highly

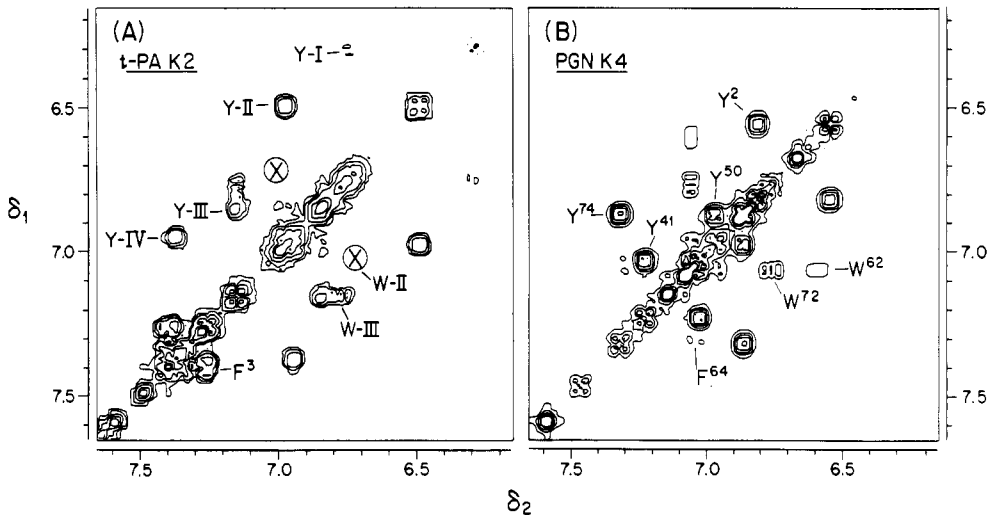

FIGURE 10: 300-MHz COSY spectra of kringle homologues: Tyr and Phe aromatic spin systems. (A) t-PA kringle 2; (B) PGN kringle 4. The assignment of aromatic signals in kringle 4 has been reported elsewhere (Trexler et al., 1985; Ramesh et al., 1986). Cross-peaks due to four Tyr residues in t-PA kringle 2 are indicated by Y-I (Tyr^{50}), Y-II (Tyr^{2}), Y-III (Tyr^{36}), and Y-IV (Tyr^{74}). Cross-peaks from the Y-V (Tyr^{9}) ring are not detected under the experimental conditions (see Figure 11). Trp cross-peaks that show in the expansion are labeled consistent with Figure 7. A broad Trp^{62} (W-II) cross-peak linking indole H7 (doublet) to H6 (triplet) resonances is marked X in spectrum A; it becomes visible in lower contour level plots or in spectra recorded at 620 MHz (not shown). Samples were dissolved in ^2H_2O, pH* 7.2; the kringle 2 solution contained 0.1 M sodium phosphate. All spectra were recorded at 37 °C; [kringle 2] ~ 0.5 mM, [kringle 4] ~ 1.5 mM.

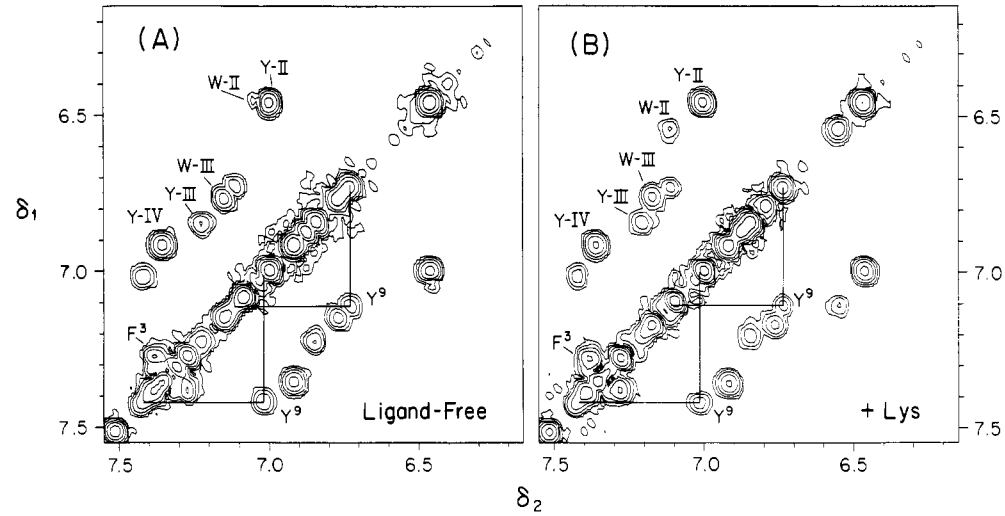

FIGURE 11: 620-MHz COSY spectra of t-PA kringle 2 in the absence (A) and presence (B) of L-Lys: Tyr and Phe aromatic region. Tyr^{9} (Y^{9}) cross-peak connectivities are indicated by solid lines; other cross-peaks are labeled consistent with Figures 7 and 10. Samples were dissolved in ^2H_2O and 0.05 M sodium phosphate, pH* 4.5, 37 °C; [kringle 2] ~ 1.5 mM. For (B), [ligand]/[kringle 2] ~ 3.

conserved throughout all kringles and suggests a structural role for this residue (Trexler & Patthy, 1983).

Phenylalanyl Spectra. t-PA kringle 2 contains a single Phe residue, located at position 3. The Phe^{3} (F^{3}) spin system can be readily identified from the characteristic connectivity pattern (Figure 10A). The chemical shift and line width of the Phe^{3} side-chain resonances are consistent with values typically exhibited by Phe residues in short, flexible peptides. Thus, the Phe^{3} side chain appears to be placed in an environment that allows for relatively unrestricted ring flip motion and is devoid of aromatic groups causing anisotropic shieldings. This is consistent with the "random coil" type aromatic spectrum of His^{3} in the human PGN kringle 4 (Ramesh et al., 1986).

Ligand-Binding Effects. Since the aromatic spin systems of t-PA kringle 2 are now assigned, it is feasible to investigate which of these residues are involved in ligand binding by simply monitoring the response of the kringle 2 spectrum to ligand additions (Ramesh et al., 1987; Motta et al., 1987; Petros et al., 1989). As is apparent from inspection of Figure 11, there are qualitative differences between aromatic COSY spectra of ligand-free (A) and ligand-bound (B) kringle 2. For example, the position of the cross-peak (δ_1 ~6.46, δ_2 ~7.05 ppm) observed for Trp^{62} (W-II) shifts to a new position (δ_1 ~6.54, δ_2 ~7.12 ppm). These spectral changes are clearly displayed in Figure 12, which shows the aromatic COSY spectrum of kringle 2 in the presence of L-Lys, superimposed on that of the ligand-free kringle. As noticed above, addition of ligand results in a major perturbation for the Trp^{62} (W-II) CH6 triplet which shifts from 7.01 to 7.30 ppm. In PGN kringle 4 the main perturbation is observed for the Trp^{62} CH7 doublet which moves from 7.09 to 6.85 ppm, a fact that is consistent with positioning this side chain at the binding site (Ramesh et al., 1987). Thus, in the t-PA kringle, the Trp^{62} side chain is most likely also located at the binding site, neighboring Asp^{57}, which is thought to provide the anionic center that interacts with the ligand ϵ-amino group (Trexler et al., 1982; Tulinsky et al., 1988a). Resonances from Tyr^{36} (Y-III), Trp^{72} (W-III), and Tyr^{74} (Y-IV) shift as well, while those from Tyr^{2} (Y-II), Phe^{3}, and Tyr^{50} (Y-I) are, at most, only slightly per-

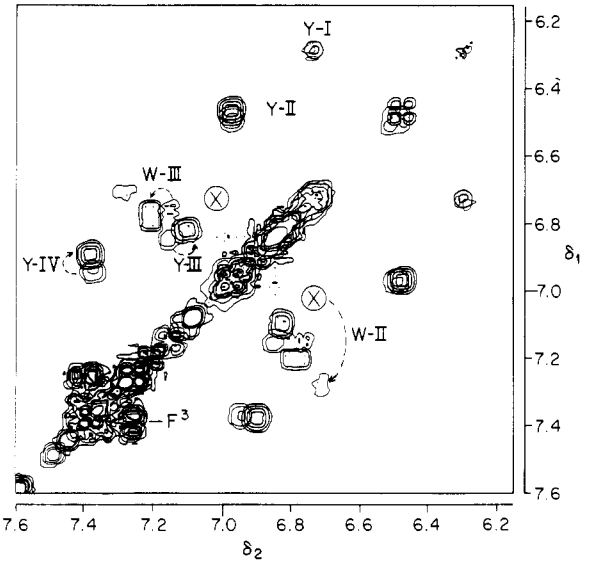

FIGURE 12: 300-MHz COSY spectra of t-PA kringle 2: ligand effects on the aromatic resonances. The spectrum of kringle 2 in the presence of L-Lys (heavy trace) is superimposed on that in the absence of ligand (thin trace). Tyr and Trp cross-peaks are labeled as in Figures 7 and 10. Arrows (dashed lines) denote ligand-induced shifts. kringle 2 concentration ~ 0.5 or 1.5 mM for spectra recorded in the absence or presence of L-Lys, respectively; for the latter, [ligand]/[kringle 2] ~ 3. Samples were dissolved in ^2H_2O and 0.1 M sodium phosphate, pH* 7.2, 37 °C.

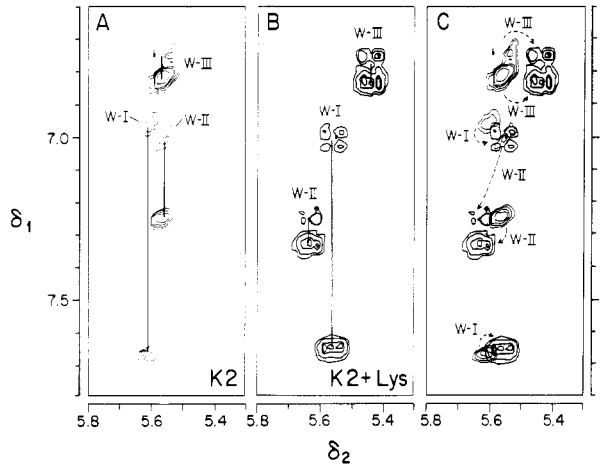

FIGURE 13: 300-MHz COSY spectra of t-PA kringle 2: ligand effects on shifted Trp indole resonances. (A) [Kringle 2] ~ 0.5 mM, in the absence of ligand; (B) [kringle 2] ~ 1.5 mM, in the presence of L-Lys; (C) superposition of spectra A and B. Spectra are resolution enhanced with Gaussian (A) or sine bell (B) filtering. Labeling of spin systems (W-I = Trp^{25}, W-II = Trp^{62}, and W-III = Trp^{72}) is consistent with Figure 7B. Cross-peaks arising from the same indole ring are shown connected with solid vertical lines. Arrows (dashed lines) indicate ligand-induced shifts. Samples were dissolved in ^2H_2O and 0.1 M sodium phosphate, pH* 7.2, 37 °C.

turbed by ligand. The ligand sensitivity of Tyr^{36} is analogous to what has been observed for the ring spin system of the site 36 residue, Phe^{36}, in PGN kringle 1 which, combined with other evidence, justified its placement at the ligand-binding site (Motta et al., 1987). Finally, the high-field aromatic spectral region of the COSY experiment (Figure 13) is consistent with these results as it reveals pronounced ligand-induced shifts for Trp^{62} (W-II) and Trp^{72} (W-III) cross-peaks, while the Trp^{25} (W-I) resonances experience only moderate perturbations.

Figure 14 shows a plot of $\Delta\delta$, the normalized chemical shift induced by L-Lys, versus $[S_0]/[K_0]$, the concentration ratio

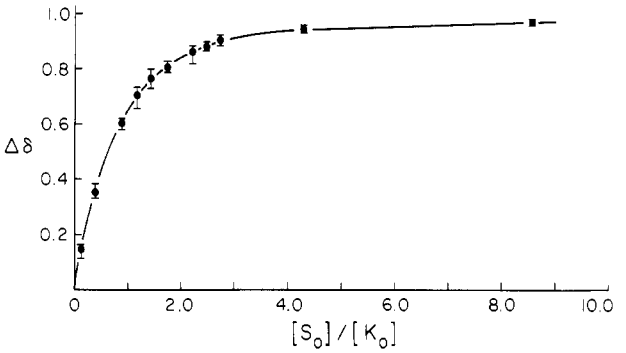

FIGURE 14: L-Lys titration profile of t-PA kringle 2. The graph plots the normalized $\Delta\delta$ (averaged over four aromatic singlets) versus $[S_0]/[K_0]$, the total ligand to total kringle concentration ratio. Kringle 2 was dissolved to ~0.4 mM in ^2H_2O and 0.1 M sodium phosphate, pH* 7.2, 22 °C.

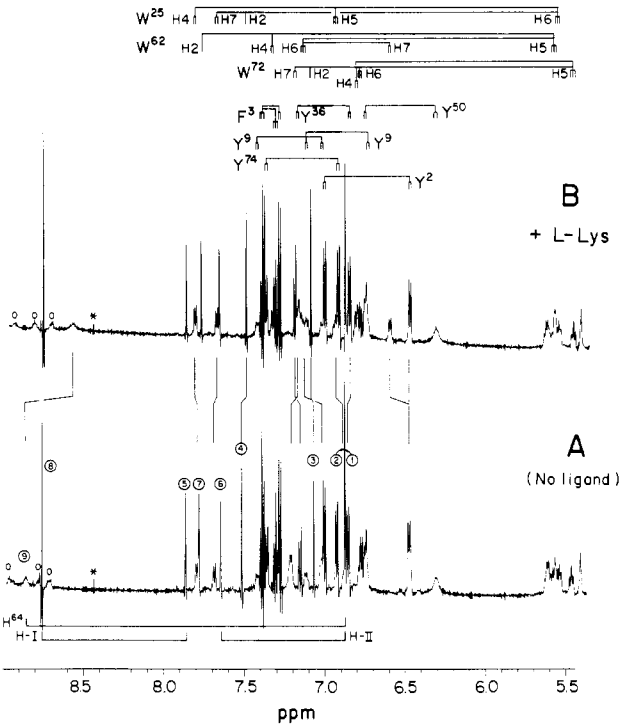

FIGURE 15: 620-MHz ^1H NMR spectra of the t-PA kringle 2: summary of aromatic resonance assignments. The spectrum of ligand-free kringle 2 (A) is compared with that of the kringle in the presence of L-Lys (B); [L-Lys]/[kringle 2] ~ 3. His and Trp singlets are labeled according to the numbering used in Figure 5. His spin systems are indicated underneath spectrum A; other assigned aromatic spin systems are indicated on top of spectrum B. The shifts induced on aromatic kringle 2 resonances by the ligand are indicated by kinked vertical lines. Kringle 2 concentration was ~ 1.5 mM, dissolved in ^2H_2O and 0.05 mM sodium phosphate, pH* 4.5, 37.8 °C. An open circle (O) is used to indicate signals arising from residual, slowly exchanging amide NH protons. An asterisk (*) denotes contaminant signals.

of total ligand to total kringle. Assuming single-site binding and fast exchange averaging of the various resonances (De Marco et al., 1982), the titration data yield $K_a = 11.9 \pm 0.4$ mM^{-1} at pH* 7.2, 22 °C. This result is in excellent agreement with equilibrium dialysis experiments which yield $K_a = 10$ mM^{-1} at pH 8, 23 °C (Cleary et al., 1989). Compared with the affinity exhibited by the PGN kringle 4 for the same ligand ($K_a = 24.4$ mM^{-1}, at pH* 7.2, 22 °C), the affinity of t-PA kringle 2 to L-Lys is about half that of PGN kringle 4. The difference must reflect slight variations in binding site structures for the two kringles as suggested by the preference of

Table I: Aromatic Resonances of t-PA Kringle 2 at pH* 7.2

residue type	spin system	ligand[a]	chemical shift (ppm)[b] H2[c]	H3[c]	H4	H5	H6	H7	assignment
tryptophan[d]	W-I	−	7.485		7.790	6.949	5.598	7.670	Trp^{25}
		+	7.449		7.814	7.025	5.556	7.661	
	W-II	−	7.676		7.249	5.564	7.010	6.728	Trp^{62}
		+	7.744		7.345	5.623	7.298	6.714	
	W-III	−	6.981		6.815	5.560	6.781	7.150	Trp^{72}
		+	7.093		6.851	5.432	6.720	7.206	
tyrosine	Y-I[e]	−	6.310	6.737					Tyr^{50}
		+	6.311	6.738					
	Y-II[e]	−	6.499	6.974					Tyr^{2}
		+	6.484	6.982					
	Y-III[e]	−	7.150	6.854					Tyr^{36}
		+	7.101	6.835					
	Y-IV[e]	−	7.368	6.949					Tyr^{74}
		+	7.379	6.902					
	Y-V[f]	−							Tyr^{9}
		+	7.345	6.917		6.761	7.101		
phenylalanine	F-I	−	7.260	7.394	7.313				Phe^{3}
		+	7.262	7.392	7.310				
histidine	H-I	−	7.851		7.581				His^{13}
		+	7.850		7.610				
	H-II	−	7.631		6.842				His^{48a}
		+	7.653		6.842				
	H-III	−	8.180		6.781				His^{64}
		+	7.981		6.816				

[a] In the absence (−) or in presence (+) of L-Lys; [ligand]/[kringle 2] ~ 3. [b] Chemical shifts measured at 620 MHz, 37.8 °C. Samples were dissolved in ^2H_2O, 50 mM sodium phosphate. [c] Except for Tyr^9, the Tyr and Phe chemical shift correspond to the averaged ortho (H2,6; column H2) or meta (H3,5; column H3) resonances. [d] Assignments of Trp aromatic resonances to specific indole protons are based on the Overhauser experiments depicted in Figure 8. [e] Ortho (H2,6) and meta (H3,5) Tyr phenol ring resonance identification is based on a NOESY experiment where cross-peaks between ortho ring proton and β-protons from the same Tyr side chain can be observed. [f] Tyr^9 signals are too broad to be identified in the absence of ligand, but they are distinct in the presence of L-Lys as four one-proton doublets. Ortho (H2, H6) and meta (H3, H5) Tyr phenol ring resonance identification is tentative, based on the "random coil" pattern whereby the H2,6 doublet appears at a lower field position relative to the H3,5 doublet.

t-PA kringle 2 for 7-aminoheptanoic acid (Cleary et al., 1989) while PGN kringle 4 exhibits a higher affinity for 6-aminohexanoic acid, a shorter ligand analogue (Winn et al., 1980).

Conclusions

In this paper we report a first NMR structural characterization of human t-PA kringle 2. Although quite different methods have been used to obtain PGN kringle 4 (proteolytic fragmentation of PGN) and the t-PA kringle 2 (recombinant techniques), a comparison of their NMR spectra indicate that the two kringles have very similar conformations. This result further supports the notion that kringles are independent structural and folding units (Castellino et al., 1981; Trexler & Patthy, 1983). The similarities among kringle spectra have enabled us to unambiguously assign most of the aromatic spin systems of t-PA kringle 2. These include Trp^{25}, Trp^{62}, Trp^{72}, Tyr^2, Tyr^9, and Tyr^{74}. The assignments of Tyr^{36}, Tyr^{50}, and His^{64} resonances were guided by homology arguments and by observing their individual responses to ligand. The assignment of His^{64} has been based on comparison with the spectrum observed for the H64Y mutant. Identification of the other two His aromatic spin systems, H-I and H-II, as arising from His^{13} and His^{48a}, respectively, has been confirmed by a sequential spectral analysis currently in progress.

Figure 15 summarizes the complete, fully identified aromatic spin systems of t-PA kringle 2, ligand free and complexed to L-Lys, at pH* 4.5. Table I lists the aromatic chemical shifts at pH* 7.2. In the aliphatic spectrum, we have also identified the $CH_3^{\delta,\delta'}$ doublets of Leu^{46} and the CH_3^{ϵ} singlet of Met^{28}. It should be noted that, despite their overall spectral similarity, chemical shifts of some aromatic side chains of t-PA kringle 2 differ somewhat from those observed for PGN kringle 4. Especially, Tyr^{50} ring protons resonate at a markedly high-field-shifted position. The observation of a strong dipolar interaction of Tyr^{50} with His^{48a} (His-II) and Trp^{25} suggests that the shifts observed for these resonances are likely to arise from the anisotropic shielding of the neighboring aromatic side chains. Such contacts would indicate that t-PA kringle 2 has essentially the same hydrophobic core—which involves the strictly conserved Leu^{46} side chain—as found in the PGN kringles (De Marco et al., 1985a; Motta et al., 1986b; Ramesh et al., 1987; Thewes et al., 1988).

We have observed that ligand addition perturbs resonances of residues similar to those that comprise the lysine-binding sites of PGN kringles, namely, Tyr^{36}, Trp^{62}, His^{64}, Trp^{72}, and Tyr^{74} (Motta et al., 1987; Ramesh et al., 1987; Tulinsky et al., 1988a). The His^{64} imidazole CH2 proton undergoes a major shift, and its ^1H–^2H exchange against the deuterated solvent slows down, in the presence of ligand. These observations suggest that His^{64} closely interacts with ligand at the binding site, which is relatively open and solvent-exposed, allowing for unhindered ligand access. This is consistent with a prediction whereby His^{64} is assigned a primary role in ligand binding by the t-PA kringle 2 (Tulinsky et al., 1988a). However, it is unlikely that ionic interactions play an important role in ligand binding by His^{64} since this residue is uncharged at pH >6 (Figure 6), which is the condition under which the ligand-binding experiment was carried out. Furthermore, site 64 is occupied by neutral residues (Tyr or Phe) in PGN kringle 1 and kringle 4 homologues which exhibit definite ligand-binding properties. Finally, the H64Y mutant kringle 2 binds ligand with approximately the same effectiveness as the wild-type domain (Kelley & Cleary, 1989b). Thus, the combined data would suggest that the aromatic residue at site 64 stabilizes ligand binding via lipophilic interactions. Nevertheless, the possibility that Tyr or neutral His at position 64 interact with the ligand carboxylate moiety in an ion–dipole fashion cannot be ruled out, since both residues contain a

H-bond donor group. Further characterization of the ligand-binding properties of t-PA kringle 2 are under investigation, and the results will be reported in due course. In the interim, the results presented in this paper afford a sound basis for a detailed NMR analysis of the evolutionary related (Patthy, 1985) u-PA kringle and t-PA kringle 1 domains.

ACKNOWLEDGMENTS

We are indebted to S. Cleary for his assistance with the kringle 2 purification.

Registry No. t-PA, 105913-11-9; L-His, 71-00-1; L-Tyr, 60-18-4; L-Trp, 73-22-3; L-Phe, 63-91-2; L-Lys, 56-87-1.

REFERENCES

Bányai, L., Váradi, A., & Patthy, L. (1983) *FEBS Lett. 163*, 37–41.

Castellino, F. J., Ploplis, V. A., Powell, J. R., & Strickland, D. K. (1981) *J. Biol. Chem. 256*, 4778–4782.

Cleary, S., Mulkerrin, M. G., & Kelley, R. F. (1989) *Biochemistry 28*, 1884–1891.

Clore, G. M., Kimber, B. J., & Gronenborn, A. M. (1983) *J. Magn. Reson. 54*, 170–173.

Collen, D. (1980) *Thromb. Haemostasis 43*, 77–89.

De Marco, A. (1977) *J. Magn. Reson. 26*, 527–528.

De Marco, A., Hochschwender, S. M., Laursen, R. A., & Llinás, M. (1982) *J. Biol. Chem. 257*, 12716–12721.

De Marco, A., Laursen, R. A., & Llinás, M. (1985a) *Biochim. Biophys. Acta 827*, 369–380.

De Marco, A., Pluck, N. D., Bányai, L., Trexler, M., Laursen, R. A., Patthy, L., Llinás, M., & Williams, R. J. P. (1985b) *Biochemistry 24*, 748–753.

De Marco, A., Petros, A. M., Laursen, R. A., & Llinás, M. (1987) *Eur. Biophys. J. 14*, 359–368.

De Marco, A., Petros, A. M., Llinás, M., Kaptein, R., & Boelens, R. (1989) *Biochim. Biophys. Acta 994*, 121–137.

Doolittle, R. F., Feng, D. F., & Johnson, M. S. (1984) *Nature 307*, 558–560.

Dubs, A., Wagner, G., & Wüthrich, K. (1979) *Biochim. Biophys. Acta 577*, 177–194.

Gething, M.-J., Adler, B., Boose, J.-A., Gerard, R. D., Madison, E. L., McGookey, D., Meidell, R. S., Roman, L. M., & Sambrook, J. (1988) *EMBO J. 7*, 2731–2740.

Glasoe, P. K., & Long, F. A. (1960) *J. Phys. Chem. 64*, 188–190.

Hochschwender, S. M., & Laursen, R. A. (1981) *J. Biol. Chem. 256*, 11172–11176.

Hochschwender, S. M., Laursen, R. A., De Marco, A., & Llinás, M. (1983) *Arch. Biochem. Biophys. 223*, 58–67.

Hoylaerts, M., Rijken, D. C., Lijnen, H. R., & Collen, D. (1982) *J. Biol. Chem. 257*, 2912–2919.

Kelley, R. F., & Cleary, S. (1989a) *Biochemistry 28*, 4047–4054.

Kelley, R. F., & Cleary, S. (1989b) 18th UCLA Symposium on Molecular and Cellular Biochemistry, *J. Cell. Biochem., Suppl. 13A*, 72 (Abstract A223).

Llinás, M., De Marco, A., Hochschwender, S. M., & Laursen, R. A. (1983) *Eur. J. Biochem. 135*, 379–391.

Llinás, M., Motta, A., De Marco, A., & Laursen, R. A. (1985) *J. Biosci. 8 (Suppl.)*, 121–139.

Mabbutt, B. C., & Williams, R. J. P. (1988) *Eur. J. Biochem. 170*, 539–548.

Markley, J. L. (1975) *Acc. Chem. Res. 8*, 70–80.

Motta, A., Laursen, R. A., & Llinás, M. (1986a) *Biochemistry 25*, 7924–7931.

Motta, A., Laursen, R. A., Rajan, N., & Llinás, M. (1986b) *J. Biol. Chem. 261*, 13684–13692.

Motta, A., Laursen, R. A., Llinás, M., Tulinsky, A., & Park, C. H. (1987) *Biochemistry 26*, 3827–3836.

Park, C. H., & Tulinsky, A. (1986) *Biochemistry 25*, 3977–3982.

Patthy, L. (1985) *Cell 41*, 657–663.

Pennica, D., Holmes, W. E., Kohr, W. J., Harkins, R. N., Vehar, G. A., Ward, C. A., Bennett, W. F., Yelverton, E., Seeberg, P. H., Heyneker, H. L., & Goeddel, D. V. (1983) *Nature (London) 301*, 214–221.

Petros, A. M., Gyenes, M., Patthy, L., & Llinás, M. (1988a) *Eur. J. Biochem. 170*, 549–563.

Petros, A. M., Gyenes, M., Patthy, L., & Llinás, M. (1988b) *Arch. Biochem. Biophys. 264*, 192–202.

Petros, A. M., Ramesh, V., & Llinás, M. (1989) *Biochemistry 28*, 1368–1376.

Ramesh, V., Gyenes, M., Patthy, L., & Llinás, M. (1986) *Eur. J. Biochem. 159*, 581–595.

Ramesh, V., Petros, A. M., Llinás, M., Tulinsky, A., & Park, C. H. (1987) *J. Mol. Biol. 198*, 481–498.

Rånby, M. (1982) *Biochim. Biophys. Acta 704*, 461–469.

Rijken, D. C., Hoylaerts, M., & Collen, D. (1982) *J. Biol. Chem. 257*, 2920–2925.

Schaller, J., Moser, P. W., Dannegger-Müller, G. A. K., Rösselet, S. J., Kämpfer, U., & Rickli, E. E. (1985) *Eur. J. Biochem. 149*, 267–268.

Sottrup-Jensen, L., Claeys, H., Zajdel, M., Petersen, T. E., & Magnusson, S. (1978) in *Chemical Fibrinolysis and Thrombolysis* (Davidson, J. F., et al., Eds.) Vol. 3, pp 191–209, Raven Press, New York.

Thewes, T. (1987) Doctoral Dissertation, Carnegie Mellon University, Pittsburgh.

Thewes, T., Ramesh, V., Simplaceanu, E. L., & Llinás, M. (1987) *Biochim. Biophys. Acta 912*, 254–269.

Thewes, T., Ramesh, V., Simplaceanu, E. L., & Llinás, M. (1988) *Eur. J. Biochem. 175*, 237–249.

Trexler, M., & Patthy, L. (1983) *Proc. Natl. Acad. Sci. U.S.A. 80*, 2457–2461.

Trexler, M., Váli, Z., & Patthy, L. (1982) *J. Biol. Chem. 257*, 7401–7406.

Trexler, M., Bányai, L., Patthy, L., Pluck, N. D., & Williams, R. J. P. (1985) *Eur. J. Biochem. 152*, 439–446.

Tulinsky, A., Park, C. H., Mao, B., & Llinás, M. (1988a) *Proteins 3*, 85–96.

Tulinsky, A., Park, C. H., & Skrzypczak-Jankun, E. (1988b) *J. Mol. Biol. 202*, 885–901.

Váli, Z., & Patthy, L. (1984) *J. Biol. Chem. 259*, 13690–13694.

Van Zonneveld, A.-J., Veerman, H., & Pannekoek, H. (1986a) *J. Biol. Chem. 261*, 14214–14218.

Van Zonneveld, A.-J., Veerman, H., & Pannekoek, H. (1986b) *Proc. Natl. Acad. Sci. U.S.A. 83*, 4670–4674.

Verheijen, J. H., Caspers, M. P. M., Chang, G. T. G., de Munk, G. A. W., Pouwels, P. H., & Enger-Valk, B. E. (1986) *EMBO J. 5*, 3525–3530.

Wider, A., Macura, S., Kumar, A., Ernst, R. R., & Wüthrich, K. (1984) *J. Magn. Reson. 56*, 207–234.

Winn, E. S., Hu, S.-P., Hochschwender, S. M., & Laursen, R. A. (1980) *Eur. J. Biochem. 104*, 579–586.